© 2016. Published by The Company of Biologists Ltd | Journal of Cell Science (2016) 129, 4563-4575 doi:10.1242/jcs.194803

RESEARCH ARTICLE

Cancer cells become less deformable and more invasive with activation of β-adrenergic signaling

Tae-Hyung Kim[1,2], Navjot Kaur Gill[1], Kendra D. Nyberg[1,3], Angelyn V. Nguyen[1], Sophia V. Hohlbauch[4], Nicholas A. Geisse[4], Cameron J. Nowell[5], Erica K. Sloan[2,5,6,7,8,*] and Amy C. Rowat[1,3,7,*,‡]

ABSTRACT

Invasion by cancer cells is a crucial step in metastasis. An oversimplified view in the literature is that cancer cells become more deformable as they become more invasive. β-adrenergic receptor (βAR) signaling drives invasion and metastasis, but the effects on cell deformability are not known. Here, we show that activation of β-adrenergic signaling by βAR agonists reduces the deformability of highly metastatic human breast cancer cells, and that these stiffer cells are more invasive *in vitro*. We find that βAR activation also reduces the deformability of ovarian, prostate, melanoma and leukemia cells. Mechanistically, we show that βAR-mediated cell stiffening depends on the actin cytoskeleton and myosin II activity. These changes in cell deformability can be prevented by pharmacological β-blockade or genetic knockout of the β_2-adrenergic receptor. Our results identify a β_2-adrenergic–Ca^{2+}–actin axis as a new regulator of cell deformability, and suggest that the relationship between cell mechanical properties and invasion might be dependent on context.

KEY WORDS: β_2-adrenergic receptor, Mechanotype, Cancer, Parallel microfiltration, Cell mechanical properties, Atomic force microscopy, Invasion

INTRODUCTION

Metastasis is the leading cause of death in cancer, but the factors that drive the invasion of cancer cells are not completely understood. Activation of β-adrenergic signaling is an emerging factor that promotes metastasis and accelerates cancer progression (Le et al., 2016; Sloan et al., 2010; Thaker et al., 2006). Cancer cells express β-adrenoceptors, whose activation results in increased invasion and metastasis *in vivo* (Creed et al., 2015; Le et al., 2016); this suggests that targeting the β-adrenergic signaling pathway might be a promising strategy to slow disease progression, especially for diseases such as triple-negative breast cancer and pancreatic cancer, which are often aggressive and have few treatment options once chemoresistance develops. Inhibition of β-adrenergic signaling is an especially promising therapeutic strategy: an effective antagonist for β-adrenergic receptors (βARs) are β-blocker drugs, which are already widely used to treat cardiac disease and hypertension (Barrese and Taglialatela, 2013; Wiysonge et al., 1996). β-blockers inhibit metastasis *in vivo* (Campbell et al., 2012; Creed et al., 2015; Le et al., 2016; Sloan et al., 2010; Sood et al., 2006) and analyses of cancer patient cohort data has revealed that coincidental use of β-blockers is linked to reduced metastasis and improved survival (Barron et al., 2011; Le et al., 2016; Melhem-Bertrandt et al., 2011; Powe et al., 2010). Recent mechanistic studies show that β-adrenergic signaling modulates metastasis by driving changes in the tumor microenvironment including vascular remodeling and immune cell recruitment (Le et al., 2016; Thaker et al., 2006). βAR activation also promotes the formation of invadopodia by tumor cells, which are essential for invasion (Creed et al., 2015). Better knowledge of the physical and mechanical changes that drive cancer cells to become more invasive with β-adrenergic signaling could provide a deeper mechanistic understanding of cancer progression and identify more effective treatment strategies.

The deformability of cancer cells is associated with cell invasive behavior and might thus play a crucial role in metastasis. To leave the tumor and invade surrounding tissue, cancer cells must adhere to fibers of the extracellular matrix (Li and Feng, 2011) and move through micrometer-scale gaps or pores. Even with the aid of secreted matrix metalloproteinases (MMPs), which can increase the effective pore size of the extracellular matrix (Goldberg et al., 2007; Lutolf and Hubbell, 2005), cells must undergo substantial deformations to transit through narrow gaps that can be up to ∼10 times smaller than their own diameter (Rowe and Weiss, 2009; Wolf et al., 2013). The requirement of cells to deform during metastasis has shaped the idea that more deformable cells have higher metastatic efficiency. Indeed, breast and ovarian cancer cells that are more deformable are more invasive *in vitro* (Swaminathan et al., 2011; Xu et al., 2012), and *in situ* analysis of human breast biopsies reveals that cells from invasive cancers are more deformable compared to those from benign lesions (Plodinec et al., 2012). However, it remains unclear if β-adrenergic signaling induces changes in the deformability of cancer cells, which could also contribute to the increased invasion and disease progression that is observed with physiological or pharmacological activation of β-adrenergic signaling (Le et al., 2016; Sloan et al., 2010; Thaker et al., 2006).

Here, we hypothesize that activation of β-adrenergic signaling impacts tumor cell invasion by causing breast cancer cells to be more deformable. To model invasive breast cancer *in vitro*, we used MDA-MB-231 breast cancer cells (Creed et al., 2015; Pon et al., 2016). We used both pharmacological and genetic tools to manipulate β-adrenergic signaling in cancer cells. To determine the ability of suspended cancer cells to deform through micrometer-scale gaps, we performed microfiltration and

[1]Department of Integrative Biology and Physiology, University of California, Los Angeles 90095, USA. [2]Semel Institute for Neuroscience and Human Behavior, University of California, Los Angeles 90095, USA. [3]Department of Bioengineering, University of California, Los Angeles 90095, USA. [4]Asylum Research, an Oxford Instruments Company, Santa Barbara, CA 93117, USA. [5]Drug Discovery Biology Theme, Monash Institute of Pharmaceutical Sciences, Monash University, Parkville, Victoria 3052, Australia. [6]Division of Cancer Surgery, Peter MacCallum Cancer Centre, Melbourne, Victoria 3000, Australia. [7]UCLA Jonsson Comprehensive Cancer Center, University of California, Los Angeles 90095, USA. [8]UCLA AIDS Institute, University of California, Los Angeles 90095, USA.
*These authors contributed equally to this work

‡Author for correspondence (rowat@ucla.edu)

T.-H.K., 0000-0002-5045-4401; A.C.R., 0000-0001-5800-5320

Received 11 July 2016; Accepted 6 November 2016

Journal of Cell Science (2016) 129, 4563-4575 doi:10.1242/jcs.194803

microfluidic deformability cytometry. We also measured the Young's modulus of adhered cells with atomic force microscopy (AFM). To evaluate the mechanisms that underlie changes in cell deformability, we conducted quantitative image analysis to determine the effects on cell and nuclear size and actin cytoskeleton organization. We show that β-adrenergic signaling contributes to the deformability of cancer cells, but unexpectedly find that βAR-activated cells are less deformable than vehicle-treated cells.

RESULTS

βAR signaling reduces the deformability of cancer cells

Cell deformability is associated with the invasive behavior of cancer cells whereby less invasive cancer cells are typically observed to be less deformable than their more invasive counterparts (Guck et al., 2005; Ochalek et al., 1988; Suresh, 2007). To test the hypothesis that βAR activation contributes to invasion and metastasis by modulating cell deformability, we treated breast cancer cells with isoproterenol, a non-selective βAR agonist, and used parallel microfiltration (PMF) to measure whole-cell deformability. Although various terminologies are used to describe the relative change in cell shape that results from physical forces, including Young's modulus and compliance, here, we use the term deformability, as this method measures the relative ability of cells in suspension to deform through micron-scale pores. PMF enables analysis of cancer cells in a format that recapitulates circulation of tumor cells in the blood and lymph vasculature during metastasis. With this technique, we can assay dozens of distinct cell samples by filtering cell suspensions through membranes with 10-µm pores in a 96-well plate format. The retention of each sample, in which the final mass is expressed as a percentage of the initial mass of loaded cell suspension, reflects the number of cells that occlude the membrane pores: a higher retention indicates a larger volume of cell suspension retained in the top well, which results from a larger number of occluded pores. The probability of pore occlusion depends on the external applied pressure, cell-to-pore size ratio and cell–surface interactions, as well as the mechanical properties of cells, such as their elastic and viscous moduli (Nyberg et al., 2016; Qi et al., 2015). At a constant applied pressure and pore size, cell deformability is a major contributor to the transit of cells through pores (Shaw Bagnall et al., 2015), and thus the retention that we measure (Qi et al., 2015).

We observed that pharmacological activation of βAR signaling in breast cancer cells resulted in a concentration-dependent increase in retention (Fig. 1A). Treatment with 0.1 nM isoproterenol had no significant effect on retention, whereas with concentrations greater than 1 nM, we observed up to a twofold increase in retention (P<0.0001). At concentrations above 10 nM isoproterenol, we observed a plateau in retention levels and did not observe any further significant increase up to 1 µM isoproterenol. Accordingly, cells were treated with a submaximal concentration of isoproterenol (3 nM) in all subsequent experiments unless otherwise specified.

Although deformation of a cell through a micrometer-scale pore is dominated by cell mechanical properties (Gabriele et al., 2009; Qi et al., 2015; Shaw Bagnall et al., 2015), it is plausible that other confounding factors might influence cell retention. To address whether an increase in cell or nuclear size results in the increased retention of βAR-activated cells, we used quantitative image analysis to confirm that treatment with isoproterenol did not significantly alter the size of cells or nuclei (Fig. S1A–D) or cell shape (Fig. S1E) when cells were in a suspended state, as measured by PMF. Alternatively, it is possible that retention might increase due to cell–surface interactions (Byun et al., 2013), for example if βAR activation changes the surface properties of cancer cells to modulate electrostatic and van der Waals interactions between cells and the porous membrane. However, we determined that there was no significant difference between the adhesion of vehicle- and isoproterenol-treated cells to a silicon nitride atomic force microscope tip (Fig. S1F). Although we cannot exclude that cells might adhere differently to the polycarbonate membrane of our PMF assay, we minimized cell–surface interactions by using bovine serum albumin (BSA) to passivate the membrane prior to filtration. Therefore, our results suggest that the effect of βAR signaling on retention is due to decreased cell deformability.

To independently confirm the effect of β-adrenergic signaling on cell deformability, we used microfluidic deformability cytometry to track the timescale for single cells to deform through a constricted channel. Stiffer cells have longer transit times, whereas more deformable cells transit through the constricted channels more quickly (Hoelzle et al., 2014). Our results showed that isoproterenol significantly increased the median transit time by 3.2-fold (P<0.01) (Fig. 1B,C), substantiating that β-adrenergic signaling causes these breast cancer cells to become less deformable.

We then determined the mechanical properties of cells in an adhered state, to model the effect of βAR signaling on tumor cells that adhere to a substrate during invasion. We used AFM to measure the Young's modulus of the cytoplasmic region of βAR-activated cells that were seeded on a Matrigel-coated substrate. Our results reveal that adhered cells also show increased resistance to deformation with a 1.8-fold higher median Young's modulus when treated with isoproterenol compared to vehicle-treated cells (P<0.01) (Fig. 1D,E). These results provide independent confirmation that βAR signaling increases the stiffness of breast cancer cells.

To verify that isoproterenol treatment activates β-adrenergic signaling in the cells that are less deformable, we assayed cAMP levels. In cancer cells, β-adrenoceptors activate adenylyl cyclase, which results in accumulation of cAMP (Mukherjee et al., 1976; Pon et al., 2016). As shown in Fig. 1F, we observed elevated cAMP levels with increasing concentrations of isoproterenol (P=0.033 at 3 nM and P<0.0001 at and above 10 nM), consistent with our previous findings (Pon et al., 2016). The isoproterenol-induced increase in cAMP followed a similar trajectory to cell retention, suggesting that β-adrenergic signaling concomitantly induces changes in cAMP levels and cell deformability. We also found that increasing levels of cAMP by treatment with forskolin, which directly activates adenylate cyclase to accumulate cAMP, is sufficient to trigger a similar increase in retention (P<0.05) (Fig. 1G). To further confirm that the effects of isoproterenol are mediated through βARs, we treated cells with propranolol, a non-selective βAR antagonist that blocks the action of isoproterenol at the receptor. We found that propranolol blocked the effects of isoproterenol on cell retention (P<0.01) (Fig. 1H), but itself had no effect (P>0.5) (Fig. 1H,I). To investigate whether the effect of βAR on cell deformability can be generalized to other cancer cell types, we used PMF to measure the effect of isoproterenol treatment on the retention of other solid tumor and blood cancer cell lines. Although the magnitude of the change in cell retention varied, isoproterenol consistently increased the retention of ovarian cancer (SK-OV-3, OVCAR-5), prostate cancer (DU-145), melanoma (LOX-IMVI) and leukemia (HL-60) cells (Fig. 1J), suggesting that these cells also become less deformable with βAR activation. Taken together, our findings suggest that signaling through the βAR modulates the cell mechanical phenotype to result in less-deformable cancer cells.

Journal of Cell Science

Journal of Cell Science (2016) 129, 4563-4575 doi:10.1242/jcs.194803

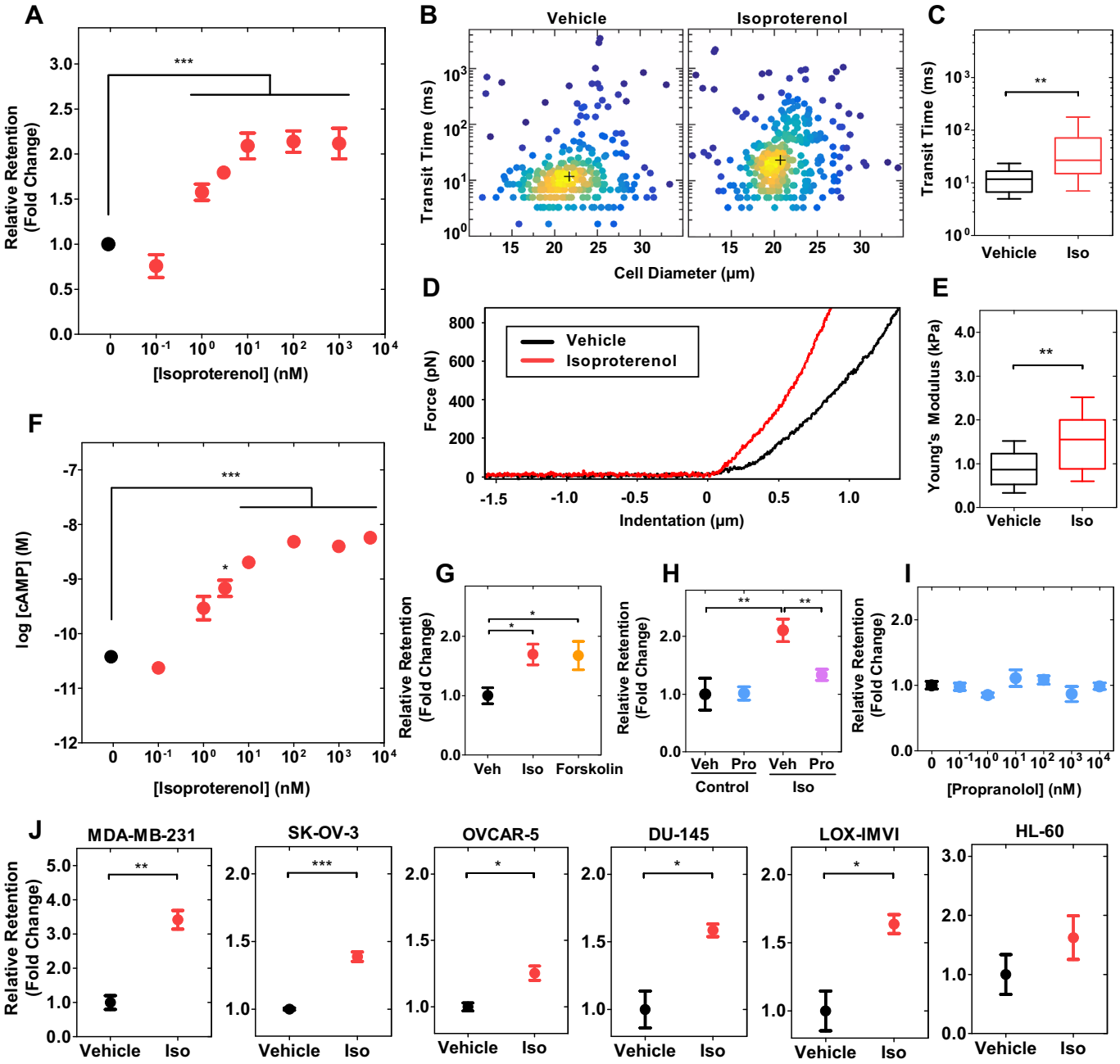

Fig. 1. Activation of βAR signaling reduces the deformability of cancer cells. (A) Relative retention of MDA-MB-231 cells measured by parallel microfiltration (PMF) and normalized to the vehicle (water) treatment after treating with varying concentrations of isoproterenol (n>5). (B) Density scatterplot showing transit time and cell size from microfluidic deformability cytometry. The crossmark indicates the median transit time and median cell size for each sample. (C) Transit time for cells to pass through the 9 μm×10 μm channel of a microfluidic device (n>59). Unless otherwise stated, the box plot shows the lower and upper quartiles with median (line). The whiskers show the 10–90th percentiles. (D) Representative force curves from AFM measurements. Force curves are fitted to the Hertz–Sneddon model and histograms of Young's moduli are shown in Fig. S2A,B. (E) Young's moduli of cells adhered to Matrigel-coated plates (n>15). (F) cAMP levels after treatment with increasing concentrations of isoproterenol (n=3). (G) Relative retention of cells after treatment with agonists (n=4). (H) Relative retention of cells measured by PMF after treatment with vehicle, isoproterenol, propranolol, and co-treatment with isoproterenol and propranolol (n=2). (I) Relative retention of cells after treatment with different concentrations of propranolol (n=2). (J) Relative retention across various cancer cell lines after isoproterenol treatment (n=3). All treatments are for 24 h prior to measurement. Owing to the variability in baseline retention from day to day, we show here data that is normalized to the vehicle control (see Fig. S1J–L for non-normalized data). Unless otherwise stated, all error bars represent mean±s.e.m. Iso, isoproterenol; Pro, propranolol; Veh, vehicle. *P<0.05; **P<0.01; ***P<0.001 [one-way ANOVA with Tukey's test (A,F,G,H,I), Mann–Whitney test (C,E) or unpaired t-test (J)].

βAR activation increases cell invasion and migration

As stiffer cancer cells are typically less invasive than more deformable cancer cells (Xu et al., 2012), we next assayed cell invasive behavior. We performed transwell migration assays, where we determined the number of cells that invade through a membrane with 8-μm pores coated with a layer of Matrigel, which simulates the extracellular matrix (Fig. 2A). We found a higher number of isoproterenol-treated cells invaded compared to the vehicle-treated cells (P=0.245) (Fig. 2B,C), suggesting that βAR-activated cells can more readily invade through a Matrigel protein matrix.

Journal of Cell Science (2016) 129, 4563-4575 doi:10.1242/jcs.194803

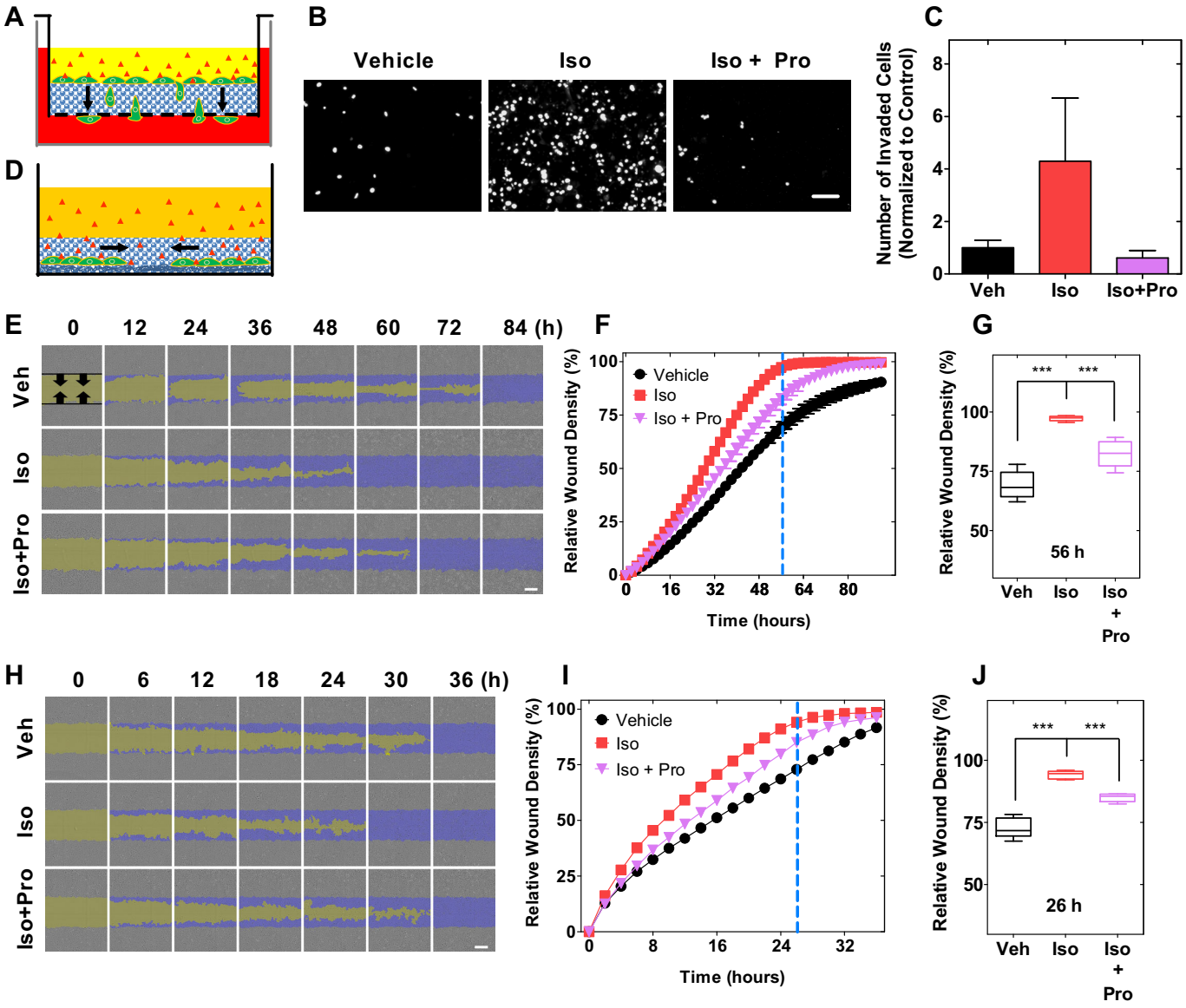

Fig. 2. Activation of βAR signaling enhances cell invasion and migration. (A) Illustration showing 3D invasion of cells in a transwell migration assay (black arrow, direction of cell invasion; blue, Matrigel; yellow, serum-free medium; red, high-serum medium; green, cells; red triangles, isoproterenol). (B) Representative images used to quantify the number of invaded cells in the transwell migration assay. Scale bar: 100 µm. (C) Quantification of the number of invaded cells normalized to that in the vehicle treatment (n=3). (D) Illustration of the modified 3D scratch wound healing assay (orange, cell culture medium; blue, Matrigel; green, cells; red triangles, isoproterenol). (E) Scratch wound invasion assay of MDA-MB-231 cells through Matrigel (black arrows, direction of cells moving into the scratch wound; yellow, initial scratch wound area; purple, area that is confluent with cells). Scale bar: 300 µm. (F,G) Relative wound density as a function of time (n=3) (F). The dashed blue line indicates the time point (56 h) that is shown in G. (H) Scratch wound migration assay of MDA-MB-231 cells on a tissue-culture treated 2D plastic substrate. Scale bar: 300 µm. (I,J) Relative wound density as a function of time (n=3) (I). The dashed blue line indicates the time point (26 h) that is shown in J. All error bars represent mean±s.e.m.; the box plots show the lower and upper quartiles with median (line), with the whiskers representing the 10–90th percentiles. Iso, isoproterenol; Pro, propranolol; Veh, vehicle. ***P<0.001 (one-way ANOVA with Tukey's test).

To confirm these findings using an independent assay, we used a modified 3D scratch wound invasion assay where breast cancer cells invaded through the interstitial gaps of Matrigel (Fig. 2D). After inducing the wound and overlaying the gap with a ∼1.5-mm-thick layer of Matrigel, we investigated the effect of isoproterenol treatment on invasion by measuring the density of cells in the wound site at 2-h intervals. We observed that isoproterenol-treated cells invaded into and filled the entire wound area by 56 h; in contrast, the vehicle-treated cells filled only 69±3% of the wound area at the same time point (mean±s.e.m; P<0.0001) (Fig. 2E–G); these results indicate the increased invasive capacity of βAR-activated cells. To confirm the role of βAR signaling in cell invasion, we blocked βARs by co-treating cells with isoproterenol and the β-antagonist propranolol; this reduced the increased invasive activity induced by isoproterenol and substantiates that βAR signaling is involved in both altered cell deformability and invasive behavior.

To assess the extent to which the increased invasive potential we observed with isoproterenol treatment was due to altered motility, we performed a scratch wound migration assay on a 2D substrate in the absence of a 3D protein network (Kramer et al., 2013). Compared to the vehicle-treated cells, isoproterenol-treated cells exhibited 29±6% faster migration on a 2D substrate (P<0.001)

Journal of Cell Science (2016) 129, 4563-4575 doi:10.1242/jcs.194803

(Fig. 2H–J). These results indicate that the increased motility of the βAR-activated cells might contribute to their increased invasive potential. The effect of βAR signaling on invasion and migration might be due to increased cell proliferation, which would allow more rapid filling of the wound gap. However, we determine that the rate of cell proliferation is not altered with isoproterenol or propranolol treatments (Fig. S1G), consistent with our findings for other cancer cell lines (Chang et al., 2016; Kim-Fuchs et al., 2014; Lamkin et al., 2012). Taken together, these findings suggest that the decreased cell deformability induced by isoproterenol treatment is associated with enhanced invasion and migration of cancer cells.

βAR activation increases F-actin levels

To begin to explore the molecular mechanism of altered cell deformability and motility induced by βAR signaling, we first evaluated the effects of filamentous (F)-actin. The structure of cytoskeletal actin is a major determinant of cell mechanical properties in both normal (Calzado-Martín et al., 2016) and tumorigenic cells (Haghparast et al., 2013), and plays a crucial role in regulating cell motility (Charras and Paluch, 2008; Tinevez et al., 2009). To address whether βAR signaling modulates the actin cytoskeleton to mediate cancer cell deformability, we evaluated how isoproterenol affects the levels and distribution of F-actin in breast cancer cells. We used quantitative imaging flow cytometry to visualize F-actin in live cells that were in a suspended state, as in the PMF and microfluidic deformability cytometry assays. Isoproterenol treatment resulted in a 1.6-fold increase in levels of F-actin in the cortical region and throughout the entire cell, compared to vehicle-treated cells (P<0.001) (Fig. 3A–C).

To form metastases, tumor cells must invade through the extracellular matrix and colonize distant tissues, which requires that cancer cells adhere to a solid substrate. Moreover, βAR activation increased the Young's modulus of adhered cells (Fig. 1D,E). Therefore, we used confocal microscopy to investigate the effect of βAR signaling on F-actin organization in cells that are attached to a glass substrate. In contrast to cells in suspension, we observed that isoproterenol did not significantly change F-actin levels of adhered cells (Fig. S3A,B). However, isoproterenol induced the formation of protrusions of the plasma membrane, which had increased levels of F-actin compared to in vehicle-treated cells (P<0.0001) (Fig. 3D,E). To quantify the number and length of protrusions per cell, we calculated the ratio of the cell perimeter to its convex hull; isoproterenol-treated cells showed a significant increase in the perimeter-to-convex-hull ratio (P<0.001) (Fig. 3F). Such protrusions are typically generated by actin remodeling and polymerization (Chhabra and Higgs, 2007); similar changes in cell morphology with increased intracellular cAMP levels are observed in other cell types (Edwards et al., 1993; Ramakers and Moolenaar, 1998). Changes in actin remodeling might be reflected in the amounts of F- and G-actin, however, we found that there was no change in the F-actin:G-actin ratio (Fig. 3G,I). We also observed no significant changes in the levels of total actin (Fig. 3H,J) or *ACTB* and *ACTG1* transcripts, which encode β-actin and γ-actin monomer subunits (Fig. S3C). Taken together, these findings show that βAR signaling regulates the remodeling of the actin cytoskeleton, with increased levels of F-actin in suspended cells, and an increased number and length of F-actin-rich protrusions in adhered cells.

βAR regulates cell deformability through a Ca^{2+}–actin axis

Our previous results show that β_2AR activation drives a cAMP–Ca^{2+} signaling loop in cancer cells that contributes to cell invasion (Pon et al., 2016). As a ubiquitous second messenger, Ca^{2+} is implicated in many intracellular processes including actin remodeling (Li et al., 2001; Wang et al., 2010), force generation (Bers, 2000), motility (Clapham, 2007), invadopodia formation (Sun et al., 2014) and tumor progression (Monteith et al., 2012). To determine the extent to which the increased Ca^{2+} levels induced by βAR activation were associated with cell deformability, we chelated cytosolic Ca^{2+} using the cell-permeable Ca^{2+} chelator, BAPTA-AM; we then investigated the effect of isoproterenol on cell retention with PMF and on invasive behavior with the 3D scratch wound invasion assay. We observed that both the increased retention and enhanced invasive activity of isoproterenol-treated cells were abolished when Ca^{2+} was chelated by BAPTA-AM (Fig 4A, Fig. S2C,D). By contrast, BAPTA-AM had no effect on baseline retention (P=0.890) (Fig. 4A). These findings show that Ca^{2+} is implicated in the altered cell deformability that occurs upon βAR activation.

To investigate whether βAR regulation of F-actin contributes to changes in cell retention, we exposed isoproterenol-treated cells to cytochalasin D to inhibit actin polymerization. Treatment with cytochalasin D alone significantly decreased retention (P<0.0001) (Fig. 4B), which is consistent with the increased cell deformability that occurs when cytoskeletal actin is perturbed (Nyberg et al., 2016; Qi et al., 2015). In the presence of isoproterenol, we observed that treatment of cells with cytochalasin D abolished the isoproterenol-induced increase in cell retention (P<0.0001); these results suggest that reorganization of cytoskeletal actin is required for the decreased cell deformability induced by βAR activation. Thus, our data indicate that the effects of βAR signaling on cell deformability and invasive activity can be abrogated by blocking either the increase in levels of Ca^{2+} or actin polymerization.

Given that actin–myosin interactions are essential for actin remodeling, we next treated cells with blebbistatin, which inhibits non-muscle myosin II. Blebbistatin also reduces the actin crosslinking and cell contractility that contribute to cell stiffness (Martens and Radmacher, 2008; Murrell et al., 2015; Wang et al., 2001, 2002). We found that blebbistatin treatment alone resulted in a trend to increased cell retention compared to with the vehicle-treated cells (P=0.105) (Fig. 4C), which is consistent with previous findings with suspended cells, where the decreased deformability is attributed to a reduction in actin remodeling (Chan et al., 2015). To determine how myosin II activity contributes to the changes in cell retention induced with βAR-activation, we co-treated cells with blebbistatin and isoproterenol. Our results showed that blebbistatin reduced retention compared to treatment with isoproterenol alone (P=0.077) (Fig. 4C); these results suggest that myosin II activity is involved in the decreased deformability of isoproterenol-treated cells in a suspended state.

To further investigate the effects of isoproterenol on myosin-II-dependent processes, we measured the Young's modulus of adhered cells that had been treated with blebbistatin. Adhered cells establish focal adhesions that enable them to generate contractile forces that depend on myosin II activity. Upon inhibition with blebbistatin, we observed a slight decrease in Young's modulus (Fig. 4D), which is consistent with other findings (Martens and Radmacher, 2008). We also found that blebbistatin treatment decreased the effect of isoproterenol on the increased Young's modulus of adhered cells (P=0.014) (Fig. 4D), indicating that myosin II activity contributes to βAR-mediated cell stiffening. Taken together, our findings suggest that processes associated with Ca^{2+}, actin and myosin, such as actin remodeling and/or contractility, could underlie βAR regulation of cell stiffness.

Journal of Cell Science (2016) 129, 4563-4575 doi:10.1242/jcs.194803

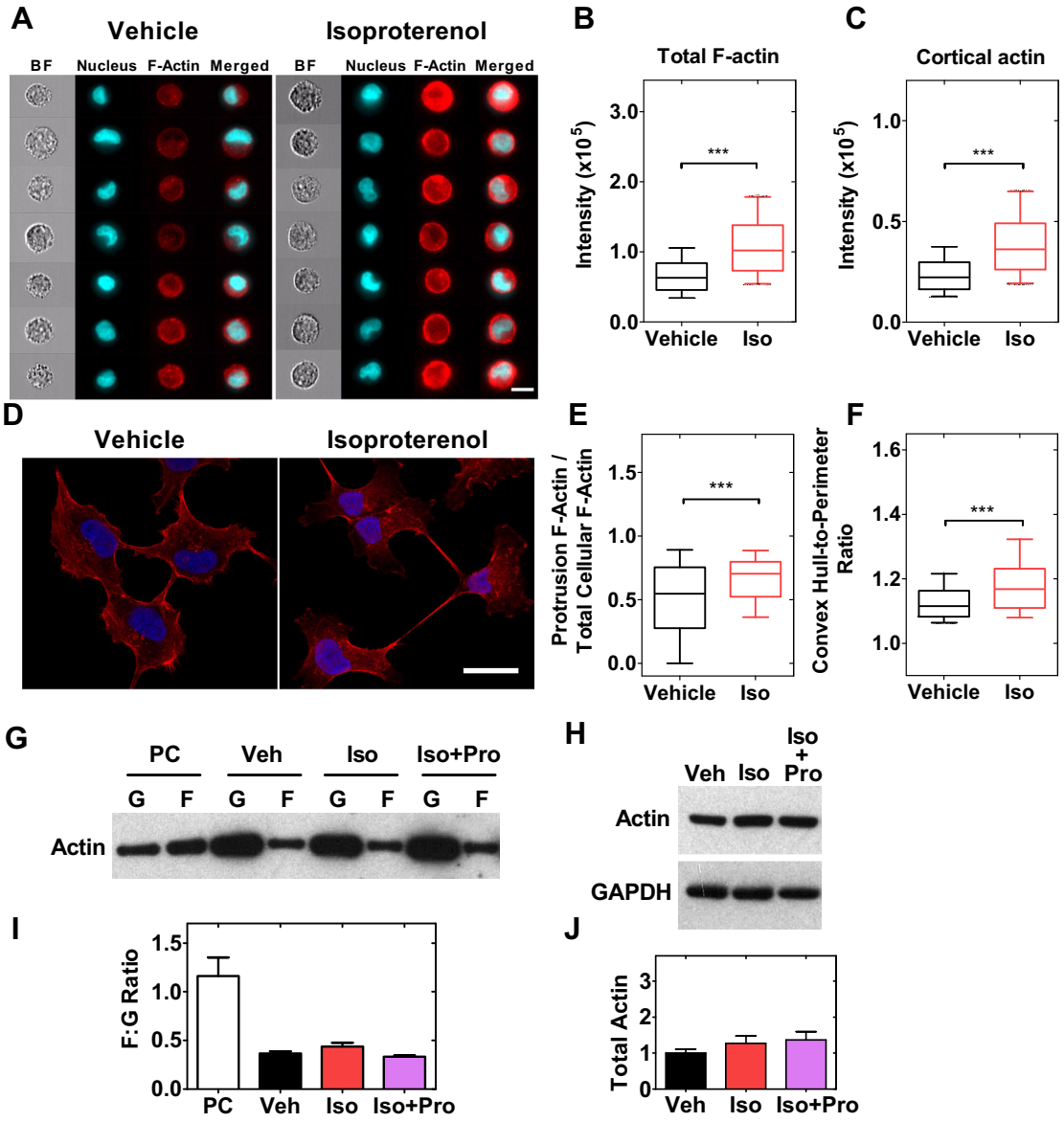

Fig. 3. Activation of βAR signaling increases cytoplasmic and cortical F-actin levels in suspended cells. (A) Representative images of live MDA-MB-231 cells in suspension obtained from imaging flow cytometry. BF, brightfield; the nucleus is labeled with Hoechst 33342 and F-actin is visualized using SiR-Actin. Scale bar: 14 µm. (B,C) Quantitative analysis showing the fluorescence intensity of (B) total F-actin and (C) cortical F-actin (n>1168). (D) Confocal images of cells that are adhered to a glass slide and stained with Phalloidin–Alexa-Fluor-546 (Red) and DRAQ5 (Cyan) to visualize F-actin and the nucleus. Scale bar: 20 µm. (E,F) Quantitative analysis of individual cells in confocal images showing (E) the ratio of F-actin intensity in protrusions to total cellular F-actin intensity (n>108) and (F) the perimeter-to-convex-hull ratio (n>283). (G) Representative image showing G- and F-actin expression levels (PC, positive control treatment with phalloidin to stabilize F-actin; G, G-actin; F, F-actin). (H) Representative images showing total actin protein levels. GAPDH is used as an internal loading control (n=2). (I) Quantification of F-actin:G-actin ratios. (J) Quantification of total actin normalized to GAPDH (n=2). Actin levels in each treatment are further normalized to vehicle treatment. All error bars represent mean±s.e.m.; the box plots show the lower and upper quartiles with median (line), with the whiskers representing the 10–90th percentiles. Iso, isoproterenol; Pro, propranolol; Veh, vehicle. ***P<0.001 [Mann–Whitney test (B,C,E,F)]. The results of Iso and Iso + Pro treatment in I and J were not statistically different from Veh control (one-way ANOVA with Tukey's test).

β_2AR mediates changes in cell deformability after isoproterenol treatment

To independently validate the effect of βAR in cancer cell deformability, we complemented our pharmacological approach with a genetic strategy to knockout the β_2AR receptor in breast cancer cells. Our previous results show that β_2AR is the only active βAR subtype in MDA-MB-231 cells (Creed et al., 2015). To delete β_2AR, we used CRISPR–Cas9 technology to mutate the *ADRB2* gene in MDA-MB-231 cells. We validated the knockout efficiency by measuring intracellular cAMP levels in four *ADRB2* knockout clones (KO-1a, 1b, 2a, and 2b that were generated from two independent guide RNAs) after treatment with isoproterenol or the β_2AR-selective agonist salmeterol. In contrast to the negative control cells, treatment of the β_2AR KO clones with either agonist resulted in no accumulation of cAMP, confirming that the *ADRB2* gene is mutated and functional receptors are absent in each of the knockout clones (Fig. 5A). To determine whether β_2AR activation resulted in altered cell deformability, we next measured the retention of *ADRB2* KO cells using PMF following treatment with isoproterenol or vehicle. Whereas negative control cells exhibited an increased

Journal of Cell Science (2016) 129, 4563-4575 doi:10.1242/jcs.194803

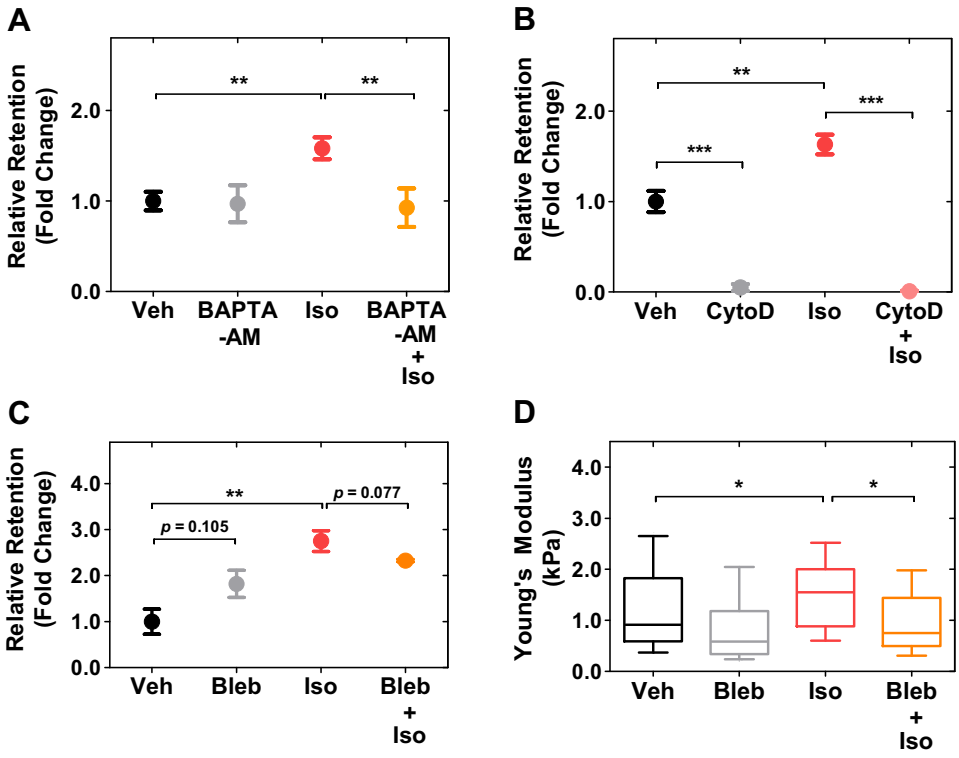

Fig. 4. The βAR-induced reduction in cell deformability depends on Ca^{2+} and actin remodeling. Relative retention of MDA-MB-231 cells measured by PMF after treatment with vehicle, BAPTA-AM, isoproterenol, and co-treatment with isoproterenol and (A) BAPTA-AM (n=3); (B) cytochalasin D (n=3); and (C) blebbistatin (n=3) (see Fig. S1M–P for non-normalized data). All data is normalized to the vehicle. (D) Young's moduli of adhered cells measured by AFM after blebbistatin treatment (n>17). All error bars represent mean±s.e.m.; the box plots show the lower and upper quartiles with median (line), with the whiskers representing the 10–90th percentiles. Iso, isoproterenol; Pro, propranolol; Veh, vehicle; Bleb, blebbistatin. *P<0.05; **P<0.01; ***P<0.001 [unpaired t-test (A,D) or one-way ANOVA with Tukey's test (B,C)].

retention after isoproterenol treatment, isoproterenol treatment did not alter the retention of the *ADRB2* KO cells (Fig. 5B). Furthermore, rescue of β_2AR in *ADRB2* KO cells restored the increased retention that we observed with isoproterenol treatment (Fig. 5C). These results provide independent confirmation that β_2AR is necessary for the isoproterenol-induced changes in cell deformability.

We next asked whether disruption of the *ADRB2* gene has functional consequences by measuring the invasive behavior of KO cells. Whereas isoproterenol treatment enhanced the invasive activity of negative control cells compared to with vehicle, we observed no significant effects of isoproterenol treatment on the invasive behavior of *ADRB2* KO cells (Figs 5D,E; Fig. S2E). Additionally, we observed that the basal invasive activity of vehicle-treated *ADRB2* KO cells was significantly lower than in the negative control cells, suggesting that β_2AR modulates cell invasion even without addition of exogenous βAR agonist. At 52 h after formation of the scratch wound, negative control cells filled 90±8% (mean±s.e.m.) of the scratch wound, whereas the *ADRB2* KO cells were significantly slower to invade Matrigel matrices, filling only 31±4% to 48±6% of the scratch wound (P<0.001) (Fig. 5D,E; Fig. S2E). Collectively, our results provide evidence that signaling through β_2AR contributes to altered invasive behavior and deformability of cancer cells.

DISCUSSION

Cell mechanotype and invasive potential

Whereas the relationship between cell deformability and higher invasive potential has been demonstrated in previous mechanotyping studies (Swaminathan et al., 2011; Xu et al., 2012), the extent to which the trend of increased deformability of cancer cells can be universally applied as a biomarker of invasion has not been well established. Here, we show that β_2AR signaling reduces the deformability of cancer cells, and this resulting stiffer mechanical phenotype is linked to increased invasion *in vitro*. These results challenge the oversimplified view that more deformable cancer cells are always more invasive. Our findings identify stress neurotransmitter signaling as a particular context where mechanotyping of tumor cells might not predict disease aggressiveness. This is important, as the deformability of malignant cells from patient pleural effusions has been suggested as an aid for pathologists to increase the accuracy of diagnosis, particularly in borderline cases (Tse et al., 2013). The findings we present here suggest that the use of cell mechanotype as a biomarker might not be appropriate for patients who are stressed at diagnosis, as indicated by elevated plasma stress neurotransmitter levels.

The β_2AR–Ca^{2+}–actin axis is a regulator of the deformability of cancer cells

Our findings that βAR signaling regulates cell deformability by remodeling the actin cytoskeleton extend our understanding of the relationship between neurotransmitter signaling and the role of the tumor cell cytoskeleton in invasion (Fig. 6). β_2AR signaling impacts tumor cell invasion by remodeling actin to form structures called invadopodia that promote cell invasion (Creed et al., 2015). β_2AR signaling also activates focal adhesion kinase (FAK, also known as PTK2), which enables adhesions with the extracellular matrix and triggers actin reorganization to drive tumor cell invasion (Sood et al., 2010). Notably FAK can also enhance cell stiffness (Fabry et al., 2011). Here, we show that β_2AR regulation of the cytoskeleton regulates cell stiffness and that this is associated with increased invasion.

Our results also highlight Ca^{2+} as a contributor to the β_2AR-induced changes in cell mechanotype. More detailed investigations will further clarify how Ca^{2+} changes that are induced by βAR signaling impact cell deformability. It is possible that the effects of Ca^{2+} on cell mechanotype might be mediated through cytoskeletal actin, whose organization and dynamics are regulated by this divalent cation (Dushek et al., 2008; Young et al., 1994). The function and activity of actin-associated proteins that regulate

Journal of Cell Science (2016) 129, 4563-4575 doi:10.1242/jcs.194803

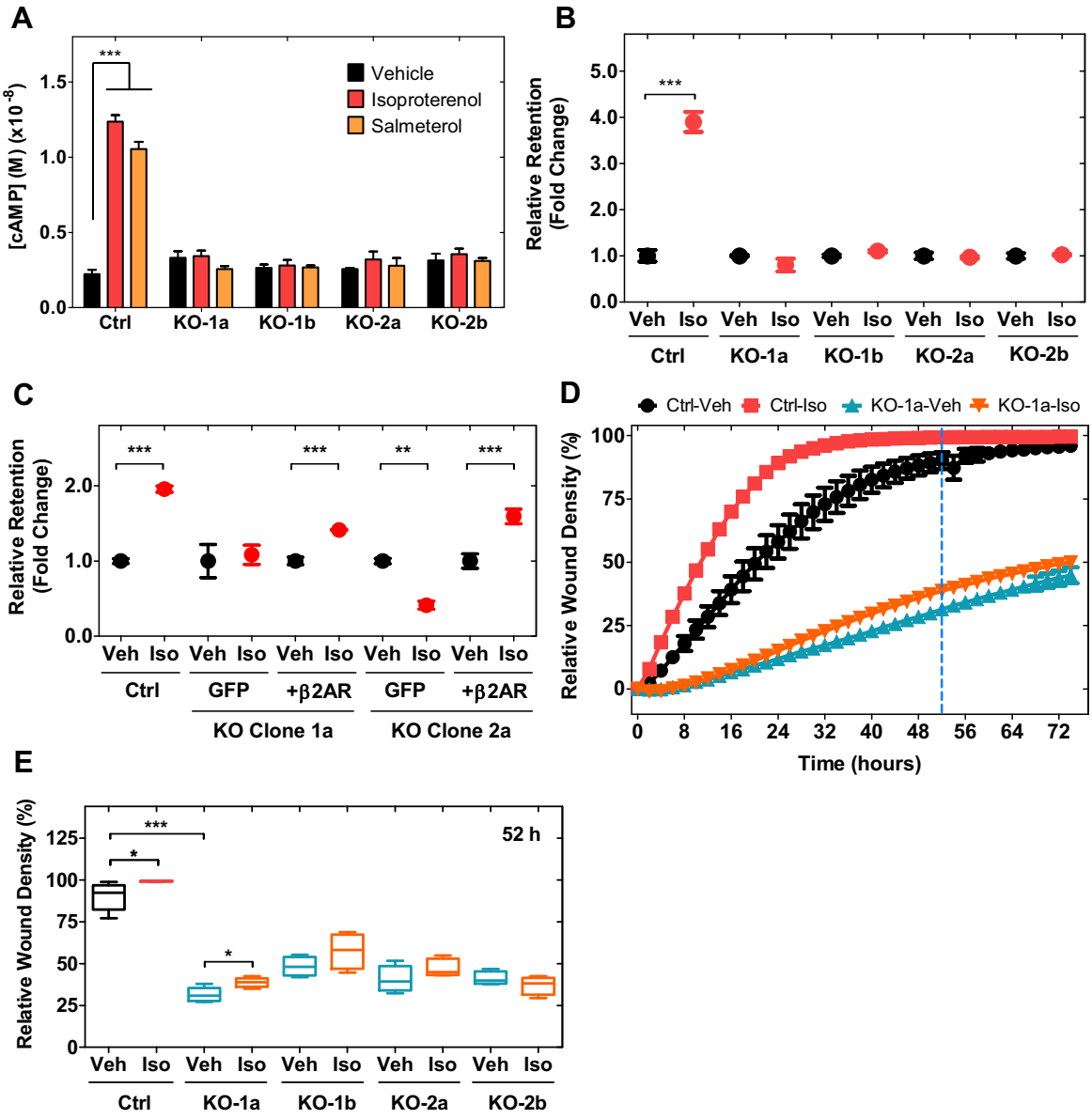

Fig. 5. Deletion of β_2AR abrogates reduced cell deformability and enhanced invasiveness with βAR activation. (A) cAMP levels after non-selective or β_2AR selective agonist treatment in parental MDA-MB-231 cells (Ctrl, negative control) and *ADRB2* KO cells (n=4). (B) Relative retention of control and KO cells measured by PMF (n=3). (C) Relative retention of KO cells after transfection with GFP or *ADRB2* (non-normalized data is displayed in Fig. S1Q,R). (D,E) Relative wound density during scratch wound invasion of control and KO-1a cells through Matrigel (n=5) (D). The dashed blue line indicates the time point (52 h) that is shown in E. All error bars represent mean±s.e.m.; the box plots show the lower and upper quartiles with median (line), with the whiskers representing the 10–90th percentiles. Iso, isoproterenol; Veh, vehicle. *P<0.05; **P<0.01; ***P<0.001 [one-way ANOVA with Tukey's test (A,B, and C) or unpaired t-test (E)].

crosslinking and severing also depend on Ca^{2+} (Furukawa et al., 2003; Witke et al., 1993; Yamamoto et al., 1982). For example, the Ca^{2+}–calmodulin complex binds to filamin, which is an actin crosslinker that regulates the cell mechanical phenotype (Kasza et al., 2009; Nakamura et al., 2005; Stossel et al., 2001). Divalent cations such as Ca^{2+} can also bind directly to actin and thereby increase the bending stiffness of actin filaments (Bidone et al., 2015) and regulate the mechanical properties of actin networks *in vitro* (Kang et al., 2012).

How is cell stiffness associated with increased invasion?

Cells that are more deformable are thought to have a selective advantage for dissemination and circulation, as they more readily transit through narrow capillaries than stiffer cells. However, our findings show that βAR signaling results in less deformable cells that are more invasive. Our results are in agreement with previous observations showing that a cell line derived from a metastatic melanoma is stiffer than cell lines derived from earlier stages in melanoma progression (Liu et al., 2015; Rathje et al., 2014; Weder et al., 2014). One possible origin of the increased stiffness in βAR-activated cells might be the altered organization of the actin cytoskeleton. We observe increased F-actin levels in suspended cells and F-actin-rich protrusions in adhered cells. Our results also indicate that non-muscle myosin II activity is implicated in βAR regulation of cell deformability. Myosin II binds to actin and regulates F-actin assembly and disassembly dynamics (Murrell

Journal of Cell Science (2016) 129, 4563-4575 doi:10.1242/jcs.194803

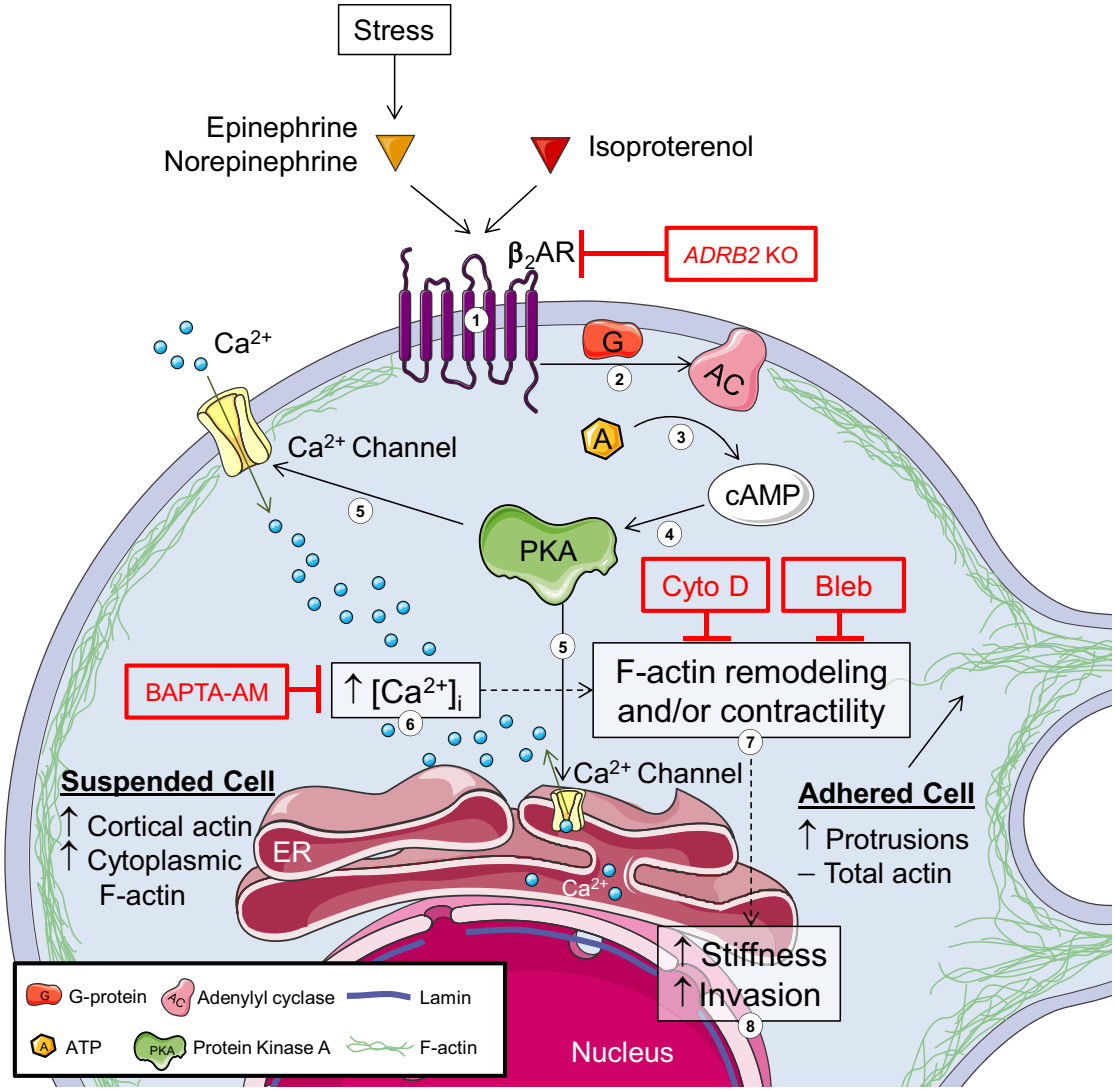

Fig. 6. Schematic illustration of putative mechanisms of how βAR may affect cell deformability and invasive activity. (1) Activation of βAR by endogenous stress neurotransmitters (epinephrine and norepinephrine) or pharmacological agonists such as isoproterenol leads to a cascade of intracellular signaling events including: (2) activation of adenylyl cyclase through G proteins; (3) production of cAMP; (4) activation of PKA by cAMP; (5) release of Ca^{2+} from the endoplasmic reticulum (ER) and import of Ca^{2+} from extracellular spaces through Ca^{2+} channels, which leads to; (6) an increased level of intracellular Ca^{2+}; (7) increased F-actin in suspended cells, and increased F-actin-rich protrusions in adhered cells, which might reflect altered actin structure. In addition, pharmacological perturbation with cytochalasin D or blebbistatin suggest that F-actin remodeling and/or contractility might occur with βAR activation. (8) Activation of βAR signaling results in increased cell invasion and reduced cell deformability. These findings build on previous characterization of signaling pathways that are activated by βAR in MDA-MB-231 cancer cells (Pon et al., 2016). Solid lines, relationships supported by the literature; dotted lines, relationships explored in our study. Images are adopted from Servier Medical Art by Servier (http://www.servier.com/Powerpoint-image-bank) and are published under published under a Creative Commons BY license (https://creativecommons.org/licenses/by-nc/3.0/). –, no change; ↑, increase.

et al., 2015), and also regulates intracellular tension (or pre-stress) and cell contractility, which can contribute to cell stiffness (An et al., 2002; Murrell et al., 2015). Indeed, cancer cells that exhibit greater traction stresses show increased invasive behavior *in vitro* (Kraning-Rush et al., 2012; Volakis et al., 2014) and *in vivo* (Paszek et al., 2005; Volakis et al., 2014).

Our results suggest that βAR signaling could enhance the contractility of cancer cells. Consistent with our observations of myosin II activity in βAR-induced cell stiffening, activation of βAR impacts the contractility of various non-transformed cell types, although not always with the same outcomes as in tumor cells. For example, βAR agonists reduce the pre-stress of airway smooth muscle cells (Wang et al., 2002). βAR agonism also increases the contractility of cardiac muscle cells (Milano et al., 1994) and skeletal muscle cells (Silva et al., 2014). Similar to our findings, βAR activation alters actin organization and migratory behavior in these cells, albeit in opposing ways: βAR agonism decreases F-actin levels in human tracheal smooth muscle cells (Hirshman et al., 2005), but inhibits the migration of human airway smooth muscle cells (Goncharova et al., 2012). It is possible that the different response of these cell types to βAR activation might be attributed to expression levels of the dominant βAR receptor subtype, or to the downstream signaling molecules that mediate the resultant phenotypic effects (Christopoulos and Kenakin, 2002). In the future, it will be important to define the relationship between patterns of βAR receptor subtype expression and cell mechanotype in different cancer subtypes, and to identify mediating signaling pathways and proteins. One candidate is cofilin, an actin-binding protein that severs and depolymerizes actin and is regulated by

Journal of Cell Science (2016) 129, 4563-4575 doi:10.1242/jcs.194803

protein kinase A (PKA) (Nadella et al., 2009). βAR regulation of PKA in tumor cells could plausibly modulate cofilin to regulate cytoskeletal dynamics, cell mechanical properties and motility (Blanchoin et al., 2000; Fan et al., 2008). Future studies will also be important to determine whether β_2AR regulation of tumor cell stiffness contributes functionally to the associated changes in cell invasion. Although it is intriguing to speculate how the cancer cell mechanotype might have functional consequences in metastasis, it is plausible that the altered mechanotype of cancer cells might be a byproduct of other genetic or signaling changes that drive invasive behavior.

βAR regulation of tumor cell deformability – adaptation to environmental cues?

Neurotransmitter signaling through βAR allows organisms to maintain homeostasis in response to a changing environment (Rockman et al., 2002). In humans and other higher organisms, βAR regulates the 'flight-or-fight' response, whereas orthologs of βAR facilitate migration in response to nutrient cues in species including *Caenorhabditis elegans* and *Drosophila melanogaster* (Bendesky et al., 2011; Carre-Pierrat et al., 2006; Koon and Budnik, 2012; Maqueira et al., 2005). During metastasis, different concentrations of catecholamines throughout the body could have distinct functional effects on tumor cell mechanotype and physical properties. For example, accumulation of endogenous epinephrine or norepinephrine in the tumor parenchyma might enable cancer cells to become stiffer and to generate increased traction forces so that they can survive and move through a stiffer extracellular matrix (Goldstein et al., 2003; Thaker et al., 2006). In situations of stress, such as during cancer diagnosis or surgery (Horowitz et al., 2015), elevated levels of catecholamines could possibly result in an increased occlusion of circulating cells and increased invasion of adhered cells into distant tissues, thereby contributing to increased metastasis. Stiffer cancer cells might be more likely to occlude the narrow capillaries of metastatic target organs such as the lung, which could enhance the probability of establishing a secondary metastatic site, and thus accelerate the spread of cancer. Future studies could define how β_2AR regulation of deformability might enable cancer cells to obtain a selective advantage for invasion and growth in secondary organs.

In vivo and clinical implications

Our study incites further *in vitro* and *in vivo* investigation of the underlying mechanisms by which β_2AR activation mediates changes in the biophysical properties of cancer cells. *In vivo* studies should help to elucidate the role of cell biophysical properties in β_2AR regulation of metastasis and in the anti-cancer effects of β-blockers. A deeper understanding of the changes in cell physical and mechanical properties, and their consequences in metastasis, might ultimately benefit the rational design of more effective drugs to inhibit disease progression.

MATERIALS AND METHODS

Cell lines and drug treatment

A highly metastatic variant of the MDA-MB-231 cells (MDA-MB-231^{HM}, a kind gift from Dr Zhou Ou, Fudan University Shanghai Cancer Center, China) (Le et al., 2016) was cultivated in Dulbecco's modified Eagle's medium (DMEM, Invitrogen) supplemented with 10% fetal bovine serum (FBS, Gemini), and 1% penicillin and streptomycin (Gibco). To investigate the effects of β-adrenergic signaling in other cancer cell types we used ovarian cancer (SK-OV-3 and OVCAR-5), prostate cancer (DU-145), melanoma (LOX-IMVI), and leukemia (HL-60) cell lines, which were all cultured in RPMI 1640 medium (Invitrogen) supplemented with 10% FBS (Gemini), and 1% penicillin and streptomycin (Gibco). Cells were maintained at 37°C with 5% CO_2. Both agonist (isoproterenol) and antagonist (propranolol) for βAR were from Sigma-Aldrich (St Louis, MO). Cells were treated for 24 h prior to measurements. For receptor blocking, cells were pre-treated with 100 nM propranolol for 20 min followed by 3 nM isoproterenol plus 100 nM propranolol treatment for 24 h. The β_2AR agonist, salmeterol (Sigma-Aldrich) was used at 100 nM. To inhibit actin polymerization, we treated cells with cytochalasin D (Santa Cruz Biotechnology) at 2 µM for 1 h. We inhibited the activity of non-muscle myosin II by treatment with 10 µM blebbistatin (Abcam) for 24 h. We activated adenylyl cyclase by treatment with 10 µM forskolin (Sigma-Aldrich) for 24 h. For Ca^{2+} chelation, we treat cells with 10 µM BAPTA-AM [1,2-Bis(2-aminophenoxy)ethane-N,N,N′,N′-tetraacetic acid tetrakis-acetoxymethyl ester; Invitrogen] for 24 h. We observed no significant changes in cell viability after BAPTA-AM treatment (Fig. S1H).

Parallel microfiltration

To measure the ability of cells to deform through micrometer-scale pores, we use parallel microfiltration (PMF) (Qi et al., 2015). Prior to the PMF assay, cells were trypsinized and filtered through a 35-µm mesh filter to reduce cell aggregates. We then counted cells using an automated cell counter (TC20, Bio-Rad) and resuspend them in medium to a density of 5×10^5 cells/ml. Membranes and inner wells of the PMF device were pretreated with 1% (w/v) BSA at 37°C for 1 h to minimize cell–surface interactions. We verified that our cell suspensions prior to filtration consisted of single cells (Fig. S1C,D); therefore, the filtration behavior is largely regulated by the occlusion of single cells rather than larger aggregates of cells. Each cell sample is measured in triplicate. Membrane pore size (5 or 10 µm), applied pressure (0.7 to 6.2 kPa), and duration of filtration (10 to 50 s) varied depending on the cell type and treatment. Retention was determined by measuring the mass of the cell suspension that remains in the top well after filtration compared to the initial mass loaded ($mass_{final}/mass_{initial}$). A population of cells that has a higher probability to occlude pores will exhibit a higher retention compared to a suspension of cells that more readily transit through pores.

Microfluidic deformability cytometry

To determine the ability of cells to passively deform through micrometer-scale gaps, we flowed cell suspensions through polydimethylsiloxane (PDMS) microfluidic devices with channels that were 9 µm×10 µm (width×height); the timescale of cell transit provides a measure of cell deformability (Hoelzle et al., 2014). We fabricated microfluidic devices using soft photolithography (Duffy et al., 1998) and bonded the PDMS to glass following corona treatment. To minimize cell–PDMS interactions, we added 0.1% (w/v) Pluronic® F-127 surfactant (Sigma-Aldrich) to the cell suspension (Wu, 2009). We flowed cell suspensions of 1.5×10^6 cells/ml through the devices using a driving pressure of 69 kPa and captured 600 frames per second using a CMOS camera mounted on an inverted DIC microscope. We performed post acquisition analysis using Matlab (Mathworks, Torrance, CA) to determine the transit time for individual cells (https://github.com/knybe/RowatLab-DC-Analysis).

Atomic force microscopy

Atomic force microscopy (AFM) was performed using the MFP-3D-BIO system (Asylum Research, Oxford Instruments). Cells were plated on a Matrigel-coated substrate (100 µg/ml). We probed cells with the 'C' tip of an MLCT probe (Bruker). The spring constant of each probe was calibrated before each experiment. Force curves were acquired by indenting the cytoplasmic region of >19 cells at room temperature. We used a constant force of 1 nN and approach and retract speeds of 5 µm/s. The Young's modulus for each cell was determined by fitting the Hertz–Sneddon model to force curves (Laurent et al., 2005) using Asylum Research software.

cAMP assay

Levels of cAMP were measured using the LANCE™ cAMP 384 kit (PerkinElmer Inc.). Cells were serum-starved overnight and pretreated with a phosphodiesterase inhibitor, IBMX (3-isobutyl-1-methylxanthine) in stimulation buffer for 30 min at 37°C; cells were then treated with agonists (isoproterenol or salmeterol) in stimulation buffer for 30 min at 37°C

followed by lysis. Cell lysates were incubated with the anti-cAMP antibody mixture included in the kit for 30 min at room temperature and the antibody is detected with a mixture of biotin–cAMP and streptavidin labeled with Europium-W8044 chelate for 1 h at room temperature. The time-resolved fluorescence resonance energy transfer (TR-FRET) signal was detected using a plate reader (Infinite® M1000, Tecan, Männedorf, Switzerland) with the following settings: 340/20 excitation (330–350 nm); 665/10 emission (660–70 nm), integration time: 200 µs, lag time, 60 µs, and settle time, 50 ms.

Invasion, migration and proliferation assay

To measure the invasive and migratory activity of cells, we used a transwell migration assay with inserts that had an 8-µm pore size. Each transwell insert (Corning) was pre-coated with 100 µl of Matrigel (2.3 mg/ml, in serum-free medium; Corning). The inserts were then placed in a 24-well plate containing 500 µl of medium with 20% serum. We then placed 100 µl of cell suspension at a density of 10^6 cells/ml in serum-free medium into the transwell. After incubation at 37°C for 24 h, we determined the number of cells that had invaded through to the bottom side of the membrane by staining with Hoechst 33342 (1 µg/ml, Invitrogen) and imaging the insert on a cover slip with a 10× objective using a fluorescence microscope (Zeiss Axio Observer.A1). We acquired ten images per transwell for at least three replicate wells for each sample. The number of invaded cells was normalized to the cell number of vehicle-treated cells.

To obtain an independent measurement of 3D cell invasion, we used a modified 3D scratch wound healing assay (Pan et al., 2016). An ImageLock 96-well plate (Essen BioScience) was pre-coated with 100 µg/ml Matrigel (Corning). We then plated 2×10^5 cells into each well and treated with drug for 24 h. We induced a scratch wound into a 100% confluent layer of cells using WoundMaker™ (Essen BioScience). Cells were then washed with medium and 8 mg/ml Matrigel was added to cover the entire well. After incubation to solidify the Matrigel, 100 µl of culture medium containing drugs was added. We acquired images every 2 h and determined the relative wound density using IncuCyte™ software (Essen BioScience). To assay 2D migration, we followed the same procedure but without the Matrigel. We also measured the proliferation of cells on Matrigel to determine any differences in doubling time due to βAR activation (a detailed description of the methods is presented in Fig. S1).

Imaging cells

To visualize F-actin in live cells in a suspended state, we stained trypsinized cells with 1 nM SiR-Actin (Cytoskeleton, Inc.) and performed imaging flow cytometry (ImageStream®X Mark II, EMD Millipore). We added Hoechst 33342 (Invitrogen) for nuclear staining. We also image F-actin in adhered cells, by fixing them with 4% paraformaldehyde, blocking with 5% (w/v) BSA in PBS with 0.3% Triton X-100, and labeling with Alexa Fluor® 546-conjugated Phalloidin (Invitrogen) and DRAQ5 (Thermo Scientific). Images were acquired using a laser-scanning confocal microscope (LSM 5, Zeiss) equipped with argon (488 and 514 nm), HeNe (543 nm) and Red Diode (633 nm) lasers and a 63× objective (NA1.2 W Corr UV-VIS-IR, C-Apochromat, Zeiss).

Image analysis

To quantify F-actin levels in suspended cells, we used the ImageStream Data Analysis and Exploration Software (IDEAS) (Amnis Corporation). The cortical region was defined by subtracting the Erode mask (8 pixel) from the Dilate mask (1 pixel) of the brightfield channel. To determine the F-actin levels in adhered cells, we used a custom script written in the Fiji distribution of ImageJ (Schindelin et al., 2012) to perform watershed segmentation. Extracted cell regions were also used to measure intensity parameters of actin. We also quantified the degree of protrusion formation by measuring the perimeter and convex hull of the cell objects to generate the convex-hull-to-perimeter ratio.

Measuring protein and transcript levels

To measure F- and G-actin protein levels, we use the G-/F-actin In Vivo Assay Biochem Kit (Cytoskeleton, Denver, CO). After ultracentrifugation of 100 µl of lysate at 100,000 ***g***, 37°C for 1 h (TLA-100 rotor, Beckman), supernatants containing G-actin were removed to fresh tubes and pellets containing F-actin were resuspended with 100 µl of F-actin depolymerization buffer. For SDS-PAGE, 8 µl of pellet and supernatant samples were loaded onto 4–12% Bolt gels (Invitrogen) with MES buffer (Invitrogen). Protein samples were transferred onto nitrocellulose membrane (GE Healthcare) with NuPAGE transfer buffer (Invitrogen). The membrane was blocked with Superblock T20 blocking buffer (ThermoFisher) followed by incubation with the following antibodies: rabbit anti-actin (#AAN01, 1:5,000; Cytoskeleton), goat anti-rabbit-IgG conjugated to horseradish peroxidase (HRP) (#sc-2004, 1:5,000; Santa Cruz Biotechnology), mouse anti-GAPDH (#MA5-15738, 1:5,000; ThermoFisher), and goat anti-mouse-IgG conjugated to HRP (#ab97240, 1:5,000; Abcam). To quantify protein levels, we measured band density using ImageJ software. To measure transcript levels of genes that encode actin, we use quantitative RT-PCR. A detailed description of the methods is presented in Fig. S3.

Gene knockout using CRISPR–Cas9

To investigate if isoproterenol treatment mediated changes in cell deformability through the β_2-adrenoceptor, we use CRISPR-Cas9 to disrupt the *ADRB2* gene in MDA-MB-231 cells. A detailed description of the method is presented in Fig. S4.

Statistical analyses

All experiments were performed at least three independent times. Statistical significance between control and treated groups was determined with a unpaired *t*-test or one-way ANOVA with Tukey's multiple comparison post hoc analysis using Graphpad Prism 5 (GraphPad Software, La Jolla, CA). To determine statistical differences between distributions, we used Mann–Whitney U tests.

Acknowledgement

The authors thank Dr Donald Lamkin and Clara Chan for technical support and critical comments on this manuscript. We thank Dr Zoran Galic for access to the ImageStream in Flow Cytometry Core Facility that is supported by the Jonsson Comprehensive Cancer Center and the Center for AIDS Research. Flow cytometry and IncuCyte analyses were performed in the Flow Cytometry Core Facility of Eli and Edythe Broad Center of Regenerative Medicine and Stem Cell Research that is supported by National Institutes of Health (awards CA-16042 and AI-28697) and the David Geffen School of Medicine at UCLA. We thank Drs Rachelle Crosbie-Watson, Emil Reisler, Elena Grintsevich, Martin Phillips, and the UCLA Biochemistry Instrumentation Core Technology Center for access to equipment for ultracentrifugation.

Competing interests

The authors declare no competing or financial interests.

Author contributions

T.-H.K., E.K.S., and A.C.R designed experiments, analyzed and interpreted data, and wrote the manuscript. T.-H.K. performed experiments presented in this manuscript. N.K.G. performed PMF and transwell migration experiments. K.D.N. performed microfluidics experiments. A.V.N., S.V.H., and N.A.G. performed atomic force microscopy experiments. C.J.N developed analytical tools for image analysis.

Funding

This work was supported by the National Institutes of Health (NIH) National Center for Advancing Translational Science (NCATS) UCLA CTSI (UL1TR000124); the National Science Foundation (CAREER DBI-1254185 to A.C.R.); the Norman Cousins Center for Psychoneuroimmunology at UCLA, and the National Cancer Institute (CA160890). Deposited in PMC for release after 12 months.

Supplementary information

Supplementary information available online at
http://jcs.biologists.org/lookup/doi/10.1242/jcs.194803.supplemental

References

An, S. S., Laudadio, R. E., Lai, J., Rogers, R. A. and Fredberg, J. J. (2002). Stiffness changes in cultured airway smooth muscle cells. *Am. J. Physiol. Cell Physiol.* **283**, C792-C801.

Barrese, V. and Taglialatela, M. (2013). New advances in beta-blocker therapy in heart failure. *Front. Physiol.* **4**, 323.

Barron, T. I., Connolly, R. M., Sharp, L., Bennett, K. and Visvanathan, K. (2011). Beta blockers and breast cancer mortality: a population- based study. *J. Clin. Oncol.* **29**, 2635-2644.
Bendesky, A., Tsunozaki, M., Rockman, M. V., Kruglyak, L. and Bargmann, C. I. (2011). Catecholamine receptor polymorphisms affect decision-making in C. elegans. *Nature* **472**, 313-318.
Bers, D. M. (2000). Calcium fluxes involved in control of cardiac myocyte contraction. *Circ. Res.* **87**, 275-281.
Bidone, T. C., Kim, T., Deriu, M. A., Morbiducci, U. and Kamm, R. D. (2015). Multiscale impact of nucleotides and cations on the conformational equilibrium, elasticity and rheology of actin filaments and crosslinked networks. *Biomech. Model. Mechanobiol.* **14**, 1143-1155.
Blanchoin, L., Pollard, T. D. and Mullins, R. D. (2000). Interactions of ADF/cofilin, Arp2/3 complex, capping protein and profilin in remodeling of branched actin filament networks. *Curr. Biol.* **10**, 1273-1282.
Byun, S., Son, S., Amodei, D., Cermak, N., Shaw, J., Kang, J. H., Hecht, V. C., Winslow, M. M., Jacks, T., Mallick, P. et al. (2013). Characterizing deformability and surface friction of cancer cells. *Proc. Natl. Acad. Sci. USA* **110**, 7580-7585.
Calzado-Martín, A., Encinar, M., Tamayo, J., Calleja, M. and San Paulo, A. (2016). Effect of actin organization on the stiffness of living breast cancer cells revealed by peak-force modulation atomic force microscopy. *ACS Nano* **10**, 3365-3374.
Campbell, J. P., Karolak, M. R., Ma, Y., Perrien, D. S., Masood-Campbell, S. K., Penner, N. L., Munoz, S. A., Zijlstra, A., Yang, X., Sterling, J. A. et al. (2012). Stimulation of host bone marrow stromal cells by sympathetic nerves promotes breast cancer bone metastasis in mice. *PLoS Biol.* **10**, e1001363.
Carre-Pierrat, M., Baillie, D., Johnsen, R., Hyde, R., Hart, A., Granger, L. and Ségalat, L. (2006). Characterization of the Caenorhabditis elegans G protein-coupled serotonin receptors. *Invert. Neurosci.* **6**, 189-205.
Chan, C. J., Ekpenyong, A. E., Golfier, S., Li, W., Chalut, K. J., Otto, O., Elgeti, J., Guck, J. and Lautenschläger, F. (2015). Myosin II activity softens cells in suspension. *Biophys. J.* **108**, 1856-1869.
Chang, A., Le, C. P., Walker, A. K., Creed, S. J., Pon, C. K., Albold, S., Carroll, D., Halls, M. L., Lane, J. R., Riedel, B. et al. (2016). β2-Adrenoceptors on tumor cells play a critical role in stress-enhanced metastasis in a mouse model of breast cancer. *Brain Behav. Immun.* **57**, 106-115.
Charras, G. and Paluch, E. (2008). Blebs lead the way: how to migrate without lamellipodia. *Nat. Rev. Mol. Cell Biol.* **9**, 730-736.
Chhabra, E. S. and Higgs, H. N. (2007). The many faces of actin: matching assembly factors with cellular structures. *Nat. Cell Biol.* **9**, 1110-1121.
Christopoulos, A. and Kenakin, T. (2002). G protein-coupled receptor allosterism and complexing. *Pharmacol. Rev.* **54**, 323-374.
Clapham, D. E. (2007). Calcium signaling. *Cell* **131**, 1047-1058.
Creed, S. J., Le, C. P., Hassan, M., Pon, C. K., Albold, S., Chan, K. T., Berginski, M. E., Huang, Z., Bear, J. E., Lane, J. R. et al. (2015). β2-adrenoceptor signaling regulates invadopodia formation to enhance tumor cell invasion. *Breast Cancer Res.* **17**, 145.
Duffy, D. C., McDonald, J. C., Schueller, O. J. A. and Whitesides, G. M. (1998). Rapid prototyping of microfluidic systems in poly(dimethylsiloxane). *Anal. Chem.* **70**, 4974-4984.
Dushek, O., Mueller, S., Soubies, S., Depoil, D., Caramalho, I., Coombs, D. and Valitutti, S. (2008). Effects of intracellular calcium and actin cytoskeleton on TCR mobility measured by fluorescence recovery. *PLoS ONE* **3**, e3913.
Edwards, J. G., Campbell, G., Carr, M. and Edwards, C. C. (1993). Shapes of cells spreading on fibronectin: measurement of the stellation of BHK21 cells induced by raising cyclic AMP, and of its reversal by serum and lysophosphatidic acid. *J. Cell Sci.* **104**, 399-407.
Fabry, B., Klemm, A. H., Kienle, S., Schäffer, T. E. and Goldmann, W. H. (2011). Focal adhesion kinase stabilizes the cytoskeleton. *Biophys. J.* **101**, 2131-2138.
Fan, X., Martin-Brown, S., Florens, L. and Li, R. (2008). Intrinsic capability of budding yeast cofilin to promote turnover of tropomyosin-bound actin filaments. *PLoS ONE* **3**, e3641.
Furukawa, R., Maselli, A., Thomson, S. A. M., Lim, R. W. L., Stokes, J. V. and Fechheimer, M. (2003). Calcium regulation of actin crosslinking is important for function of the actin cytoskeleton in Dictyostelium. *J. Cell Sci.* **116**, 187-196.
Gabriele, S., Benoliel, A.-M., Bongrand, P. and Théodoly, O. (2009). Microfluidic investigation reveals distinct roles for actin cytoskeleton and myosin II activity in capillary leukocyte trafficking. *Biophys. J.* **96**, 4308-4318.
Goldberg, M., Langer, R. and Jia, X. (2007). Nanostructured materials for applications in drug delivery and tissue engineering. *J. Biomater. Sci. Polym. Ed.* **18**, 241-268.
Goldstein, D. S., Eisenhofer, G. and Kopin, I. J. (2003). Sources and significance of plasma levels of catechols and their metabolites in humans. *J. Pharmacol. Exp. Ther.* **305**, 800-811.
Goncharova, E. A., Goncharov, D. A., Zhao, H., Penn, R. B., Krymskaya, V. P. and Panettieri, R. A. (2012). β2-adrenergic receptor agonists modulate human airway smooth muscle cell migration via vasodilator-stimulated phosphoprotein. *Am. J. Respir. Cell Mol. Biol.* **46**, 48-54.
Guck, J., Schinkinger, S., Lincoln, B., Wottawah, F., Ebert, S., Romeyke, M., Lenz, D., Erickson, H. M., Ananthakrishnan, R., Mitchell, D. et al. (2005). Optical deformability as an inherent cell marker for testing malignant transformation and metastatic competence. *Biophys. J.* **88**, 3689-3698.
Haghparast, S. M. A., Kihara, T., Shimizu, Y., Yuba, S. and Miyake, J. (2013). Actin-based biomechanical features of suspended normal and cancer cells. *J. Biosci. Bioeng.* **116**, 380-385.
Hirshman, C. A., Zhu, D., Pertel, T., Panettieri, R. A. and Emala, C. W. (2005). Isoproterenol induces actin depolymerization in human airway smooth muscle cells via activation of an Src kinase and GS. *Am. J. Physiol. Lung Cell. Mol. Physiol.* **288**, L924-L931.
Hoelzle, D. J., Varghese, B. A., Chan, C. K. and Rowat, A. C. (2014). A microfluidic technique to probe cell deformability. *J. Vis. Exp.*, **91**, e51474.
Horowitz, M., Neeman, E., Sharon, E. and Ben-Eliyahu, S. (2015). Exploiting the critical perioperative period to improve long-term cancer outcomes. *Nat. Rev. Clin. Oncol.* **12**, 213-226.
Kang, H., Bradley, M. J., McCullough, B. R., Pierre, A., Grintsevich, E. E., Reisler, E. and De La Cruz, E. M. (2012). Identification of cation-binding sites on actin that drive polymerization and modulate bending stiffness. *Proc. Natl. Acad. Sci. USA* **109**, 16923-16927.
Kasza, K. E., Nakamura, F., Hu, S., Kollmannsberger, P., Bonakdar, N., Fabry, B., Stossel, T. P., Wang, N. and Weitz, D. A. (2009). Filamin A is essential for active cell stiffening but not passive stiffening under external force. *Biophys. J.* **96**, 4326-4335.
Kim-Fuchs, C., Le, C. P., Pimentel, M. A., Shackleford, D., Ferrari, D., Angst, E., Hollande, F. and Sloan, E. K. (2014). Chronic stress accelerates pancreatic cancer growth and invasion: a critical role for beta-adrenergic signaling in the pancreatic microenvironment. *Brain Behav. Immun.* **40**, 40-47.
Koon, A. C. and Budnik, V. (2012). Inhibitory control of synaptic and behavioral plasticity by octopaminergic signaling. *J. Neurosci.* **32**, 6312-6322.
Kramer, N., Walzl, A., Unger, C., Rosner, M., Krupitza, G., Hengstschläger, M. and Dolznig, H. (2013). In vitro cell migration and invasion assays. *Mutat. Res.* **752**, 10-24.
Kraning-Rush, C. M., Califano, J. P. and Reinhart-King, C. A. (2012). Cellular traction stresses increase with increasing metastatic potential. *PLoS ONE* **7**, e32572.
Lamkin, D. M., Sloan, E. K., Patel, A. J., Chiang, B. S., Pimentel, M. A., Ma, J. C. Y., Arevalo, J. M., Morizono, K. and Cole, S. W. (2012). Chronic stress enhances progression of acute lymphoblastic leukemia via β-adrenergic signaling. *Brain Behav. Immun.* **26**, 635-641.
Laurent, V. M., Kasas, S., Yersin, A., Schäffer, T. E., Catsicas, S., Dietler, G., Verkhovsky, A. B. and Meister, J.-J. (2005). Gradient of rigidity in the lamellipodia of migrating cells revealed by atomic force microscopy. *Biophys. J.* **89**, 667-675.
Le, C. P., Nowell, C. J., Kim-Fuchs, C., Botteri, E., Hiller, J. G., Ismail, H., Pimentel, M. A., Chai, M. G., Karnezis, T., Rotmensz, N. et al. (2016). Chronic stress in mice remodels lymph vasculature to promote tumour cell dissemination. *Nat. Commun.* **7**, 10634.
Li, D.-M. and Feng, Y.-M. (2011). Signaling mechanism of cell adhesion molecules in breast cancer metastasis: potential therapeutic targets. *Breast Cancer Res. Treat.* **128**, 7-21.
Li, C., Fultz, M. E., Parkash, J., Rhoten, W. B. and Wright, G. L. (2001). Ca2 +-dependent actin remodeling in the contracting A7r5 cell. *J. Muscle Res. Cell Motil.* **22**, 521-534.
Liu, C.-Y., Lin, H.-H., Tang, M.-J. and Wang, Y.-K. (2015). Vimentin contributes to epithelial-mesenchymal transition cancer cell mechanics by mediating cytoskeletal organization and focal adhesion maturation. *Oncotarget* **6**, 15966-15983.
Lutolf, M. P. and Hubbell, J. A. (2005). Synthetic biomaterials as instructive extracellular microenvironments for morphogenesis in tissue engineering. *Nat. Biotechnol.* **23**, 47-55.
Maqueira, B., Chatwin, H. and Evans, P. D. (2005). Identification and characterization of a novel family of Drosophila beta-adrenergic-like octopamine G-protein coupled receptors. *J. Neurochem.* **94**, 547-560.
Martens, J. C. and Radmacher, M. (2008). Softening of the actin cytoskeleton by inhibition of myosin II. *Pflugers Arch.* **456**, 95-100.
Melhem-Bertrandt, A., Chavez-Macgregor, M., Lei, X., Brown, E. N., Lee, R. T., Meric-Bernstam, F., Sood, A. K., Conzen, S. D., Hortobagyi, G. N. and Gonzalez-Angulo, A.-M. (2011). Beta-blocker use is associated with improved relapse-free survival in patients with triple-negative breast cancer. *J. Clin. Oncol.* **29**, 2645-2652.
Milano, C. A., Allen, L. F., Rockman, H. A., Dolber, P. C., McMinn, T. R., Chien, K. R., Johnson, T. D., Bond, R. A. and Lefkowitz, R. J. (1994). Enhanced myocardial function in transgenic mice overexpressing the beta 2-adrenergic receptor. *Science* **264**, 582-586.
Monteith, G. R., Davis, F. M. and Roberts-Thomson, S. J. (2012). Calcium channels and pumps in cancer: changes and consequences. *J. Biol. Chem.* **287**, 31666-31673.
Mukherjee, C., Caron, M. G. and Lefkowitz, R. J. (1976). Regulation of adenylate cyclase coupled beta-adrenergic receptors by beta-adrenergic catecholamines. *Endocrinology* **99**, 347-357.

Journal of Cell Science

Murrell, M., Oakes, P. W., Lenz, M. and Gardel, M. L. (2015). Forcing cells into shape: the mechanics of actomyosin contractility. *Nat. Rev. Mol. Cell Biol.* **16**, 486-498.
Nadella, K. S., Saji, M., Jacob, N. K., Pavel, E., Ringel, M. D. and Kirschner, L. S. (2009). Regulation of actin function by protein kinase A-mediated phosphorylation of Limk1. *EMBO Rep.* **10**, 599-605.
Nakamura, F., Hartwig, J. H., Stossel, T. P. and Szymanski, P. T. (2005). Ca2+ and calmodulin regulate the binding of filamin A to actin filaments. *J. Biol. Chem.* **280**, 32426-32433.
Nyberg, K. D., Scott, M. B., Bruce, S. L., Gopinath, A. B., Bikos, D., Mason, T. G., Kim, J. W., Choi, H. S. and Rowat, A. C. (2016). The physical origins of transit time measurements for rapid, single cell mechanotyping. *Lab. Chip* **16**, 3330-3339.
Ochalek, T., Nordt, F. J., Tullberg, K. and Burger, M. M. (1988). Correlation between cell deformability and metastatic potential in B16-F1 melanoma cell variants. *Cancer Res.* **48**, 5124-5128.
Pan, Y., Robertson, G., Pedersen, L., Lim, E., Hernandez-Herrera, A., Rowat, A. C., Patil, S. L., Chan, C. K., Wen, Y., Zhang, X. et al. (2016). miR-509-3p is clinically significant and strongly attenuates cellular migration and multi-cellular spheroids in ovarian cancer. *Oncotarget* **7**, 25930-25948.
Paszek, M. J., Zahir, N., Johnson, K. R., Lakins, J. N., Rozenberg, G. I., Gefen, A., Reinhart-King, C. A., Margulies, S. S., Dembo, M., Boettiger, D. et al. (2005). Tensional homeostasis and the malignant phenotype. *Cancer Cell* **8**, 241-254.
Plodinec, M., Loparic, M., Monnier, C. A., Obermann, E. C., Zanetti-Dallenbach, R., Oertle, P., Hyotyla, J. T., Aebi, U., Bentires-Alj, M., Lim, R. Y. H. et al. (2012). The nanomechanical signature of breast cancer. *Nat. Nanotechnol.* **7**, 757-765.
Pon, C. K., Lane, J. R., Sloan, E. K. and Halls, M. L. (2016). The β2-adrenoceptor activates a positive cAMP-calcium feedforward loop to drive breast cancer cell invasion. *FASEB J.* **30**, 1144-1154.
Powe, D. G., Voss, M. J., Zänker, K. S., Habashy, H. O., Green, A. R., Ellis, I. O. and Entschladen, F. (2010). Beta-blocker drug therapy reduces secondary cancer formation in breast cancer and improves cancer specific survival. *Oncotarget* **1**, 628-638.
Qi, D., Kaur Gill, N., Santiskulvong, C., Sifuentes, J., Dorigo, O., Rao, J., Taylor-Harding, B., Ruprecht Wiedemeyer, W. and Rowat, A. C. (2015). Screening cell mechanotype by parallel microfiltration. *Sci. Rep.* **5**, 17595.
Ramakers, G. J. A. and Moolenaar, W. H. (1998). Regulation of astrocyte morphology by RhoA and lysophosphatidic acid. *Exp. Cell Res.* **245**, 252-262.
Rathje, L.-S. Z., Nordgren, N., Pettersson, T., Rönnlund, D., Widengren, J., Aspenström, P. and Gad, A. K. B. (2014). Oncogenes induce a vimentin filament collapse mediated by HDAC6 that is linked to cell stiffness. *Proc. Natl. Acad. Sci. USA* **111**, 1515-1520.
Rockman, H. A., Koch, W. J. and Lefkowitz, R. J. (2002). Seven-transmembrane-spanning receptors and heart function. *Nature* **415**, 206-212.
Rowe, R. G. and Weiss, S. J. (2009). Navigating ECM barriers at the invasive front: the cancer cell-stroma interface. *Annu. Rev. Cell Dev. Biol.* **25**, 567-595.
Schindelin, J., Arganda-Carreras, I., Frise, E., Kaynig, V., Longair, M., Pietzsch, T., Preibisch, S., Rueden, C., Saalfeld, S., Schmid, B. et al. (2012). Fiji: an open-source platform for biological-image analysis. *Nat. Methods* **9**, 676-682.
Shaw Bagnall, J., Byun, S., Begum, S., Miyamoto, D. T., Hecht, V. C., Maheswaran, S., Stott, S. L., Toner, M., Hynes, R. O. and Manalis, S. R. (2015). Deformability of tumor cells versus blood cells. *Sci. Rep.* **5**, 18542.
Silva, M. T., Wensing, L. A., Brum, P. C., Câmara, N. O. and Miyabara, E. H. (2014). Impaired structural and functional regeneration of skeletal muscles from β2-adrenoceptor knockout mice. *Acta Physiol. (Oxf.)* **211**, 617-633.
Sloan, E. K., Priceman, S. J., Cox, B. F., Yu, S., Pimentel, M. A., Tangkanangnukul, V., Arevalo, J. M. G., Morizono, K., Karanikolas, B. D. W., Wu, L. et al. (2010). The sympathetic nervous system induces a metastatic switch in primary breast cancer. *Cancer Res.* **70**, 7042-7052.
Sood, A. K., Bhatty, R., Kamat, A. A., Landen, C. N., Han, L., Thaker, P. H., Li, Y., Gershenson, D. M., Lutgendorf, S. and Cole, S. W. (2006). Stress hormone-mediated invasion of ovarian cancer cells. *Clin. Cancer Res.* **12**, 369-375.
Sood, A. K., Armaiz-Pena, G. N., Halder, J., Nick, A. M., Stone, R. L., Hu, W., Carroll, A. R., Spannuth, W. A., Deavers, M. T., Allen, J. K. et al. (2010). Adrenergic modulation of focal adhesion kinase protects human ovarian cancer cells from anoikis. *J. Clin. Invest.* **120**, 1515-1523.
Stossel, T. P., Condeelis, J., Cooley, L., Hartwig, J. H., Noegel, A., Schleicher, M. and Shapiro, S. S. (2001). Filamins as integrators of cell mechanics and signalling. *Nat. Rev. Mol. Cell Biol.* **2**, 138-145.
Sun, J., Lu, F., He, H., Shen, J., Messina, J., Mathew, R., Wang, D., Sarnaik, A. A., Chang, W.-C., Kim, M. et al. (2014). STIM1- and Orai1-mediated Ca(2+) oscillation orchestrates invadopodium formation and melanoma invasion. *J. Cell Biol.* **207**, 535-548.
Suresh, S. (2007). Biomechanics and biophysics of cancer cells. *Acta Biomater.* **3**, 413-438.
Swaminathan, V., Mythreye, K., O'Brien, E. T., Berchuck, A., Blobe, G. C. and Superfine, R. (2011). Mechanical stiffness grades metastatic potential in patient tumor cells and in cancer cell lines. *Cancer Res.* **71**, 5075-5080.
Thaker, P. H., Han, L. Y., Kamat, A. A., Arevalo, J. M., Takahashi, R., Lu, C., Jennings, N. B., Armaiz-Pena, G., Bankson, J. A., Ravoori, M. et al. (2006). Chronic stress promotes tumor growth and angiogenesis in a mouse model of ovarian carcinoma. *Nat. Med.* **12**, 939-944.
Tinevez, J.-Y., Schulze, U., Salbreux, G., Roensch, J., Joanny, J.-F. and Paluch, E. (2009). Role of cortical tension in bleb growth. *Proc. Natl. Acad. Sci. USA* **106**, 18581-18586.
Tse, H. T. K., Gossett, D. R., Moon, Y. S., Masaeli, M., Sohsman, M., Ying, Y., Mislick, K., Adams, R. P., Rao, J. and Di Carlo, D. (2013). Quantitative diagnosis of malignant pleural effusions by single-cell mechanophenotyping. *Sci. Transl. Med.* **5**, 212ra163.
Volakis, L. I., Li, R., Ackerman, W. E., Mihai, C., Bechel, M., Summerfield, T. L., Ahn, C. S., Powell, H. M., Zielinski, R., Rosol, T. J. et al. (2014). Loss of myoferlin redirects breast cancer cell motility towards collective migration. *PLoS ONE* **9**, e86110.
Wang, N., Naruse, K., Stamenović, D., Fredberg, J. J., Mijailovich, S. M., Tolić-Nørrelykke, I. M., Polte, T., Mannix, R. and Ingber, D. E. (2001). Mechanical behavior in living cells consistent with the tensegrity model. *Proc. Natl. Acad. Sci. USA* **98**, 7765-7770.
Wang, N., Tolić-Nørrelykke, I. M., Chen, J., Mijailovich, S. M., Butler, J. P., Fredberg, J. J. and Stamenović, D. (2002). Cell prestress. I. Stiffness and prestress are closely associated in adherent contractile cells. *Am. J. Physiol. Cell Physiol.* **282**, C606-C616.
Wang, Q., Symes, A. J., Kane, C. A., Freeman, A., Nariculam, J., Munson, P., Thrasivoulou, C., Masters, J. R. W. and Ahmed, A. (2010). A novel role for Wnt/Ca2+ signaling in actin cytoskeleton remodeling and cell motility in prostate cancer. *PLoS ONE* **5**, e10456.
Weder, G., Hendriks-Balk, M. C., Smajda, R., Rimoldi, D., Liley, M., Heinzelmann, H., Meister, A. and Mariotti, A. (2014). Increased plasticity of the stiffness of melanoma cells correlates with their acquisition of metastatic properties. *Nanomedicine* **10**, 141-148.
Witke, W., Hofmann, A., Köppel, B., Schleicher, M. and Noegel, A. A. (1993). The Ca(2+)-binding domains in non-muscle type alpha-actinin: biochemical and genetic analysis. *J. Cell Biol.* **121**, 599-606.
Wiysonge, C. S., Bradley, H. A., Volmink, J., Mayosi, B. M., Mbewu, A. and Opie, L. H. (2012). Beta-blockers for hypertension. *Cochrane Database Syst. Rev.* **11**, CD002003.
Wolf, K., te Lindert, M., Krause, M., Alexander, S., te Riet, J., Willis, A. L., Hoffman, R. M., Figdor, C. G., Weiss, S. J. and Friedl, P. (2013). Physical limits of cell migration: control by ECM space and nuclear deformation and tuning by proteolysis and traction force. *J. Cell Biol.* **201**, 1069-1084.
Wu, M.-H. (2009). Simple poly(dimethylsiloxane) surface modification to control cell adhesion. *Surf. Interface Anal.* **41**, 11-16.
Xu, W., Mezencev, R., Kim, B., Wang, L., McDonald, J. and Sulchek, T. (2012). Cell stiffness is a biomarker of the metastatic potential of ovarian cancer cells. *PLoS ONE* **7**, e46609.
Yamamoto, K., Pardee, J. D., Reidler, J., Stryer, L. and Spudich, J. A. (1982). Mechanism of interaction of Dictyostelium severin with actin filaments. *J. Cell Biol.* **95**, 711-719.
Young, C. L., Feierstein, A. and Southwick, F. S. (1994). Calcium regulation of actin filament capping and monomer binding by macrophage capping protein. *J. Biol. Chem.* **269**, 13997-14002.